Article

SBA-15 Loaded with Methylene Blue Dye for Efficient and Low-Cost Decontamination of Water under Visible Led Light

Khaled Chawraba , Hussein Medlej , Malak Hamieh , Jacques Lalevée , Tayssir Hamieh * , Joumana Toufaily

Posted Date: 4 April 2024

doi: 10.20944/preprints202404.0330.v1

Keywords: SBA-15; Methylene blue; sensitization; wastewater treatment; photocatalysis; visible light

Article

SBA-15 Loaded with Methylene Blue Dye for Efficient and Low-Cost Decontamination of Water under Visible LED Light

Khaled Chawraba [1,2,*], Hussein Medlej [1,2], Malak Hamieh [1,2], Jacques Lalevee [3,4], Tayssir Hamieh [1,5,*] and Joumana Toufaily [1,2]

1 Laboratory of Materials, Catalysis, Environment, and Analytical Methods Laboratory (MCEMA), Faculty of Sciences, Lebanese University, Hadath, Beirut, P.O. Box 6573/14 Badaro, Lebanon
2 LEADDER Laboratory, Faculty of Sciences and EDST, Lebanese University, Hariri Campus, Hadath, Beirut, P.O. Box 6573/14 Badaro, Beirut, Lebanon
3 CNRS, IS2M UMR 7361, University of Haute-Alsace, 68100 Mulhouse, France
4 University of Strasbourg, 67081 Strasbourg, France
5 Faculty of Science and Engineering, Maastricht University, P.O. Box 616, 6200 MD Maastricht, The Netherlands
* Correspondence: Khaled.chawraba.1@ul.edu.lb (K.C.); t.hamieh@maastrichtuniversity.nl (T.H.)

Abstract: The SBA-15 loaded with methylene blue was successfully prepared by sample adsorption of methylene blue in SBA-15 and is characterized by an XRD, SEM, FTIR, and BET. The photocatalytic activity for methyl orange (MO) degradation was investigated under visible light irradiation under LEDs. Experimental results demonstrate that the SBA-15-MB exhibited higher photocatalytic activity than SBA-15 under visible light irradiation. The degradation efficiency of MO (50 ppm) by SBA-15-MB could reach 80% within 180 min under 25W LED visible light. The photocatalytic activity of SBA-15 could be attributed to the excitation of methylene blue by visible light, the transfer of electrons from methylene blue to SBA-15, and the production of radicals at the surface of SBA-15.

Keywords: SBA-15; methylene blue; sensitization; wastewater treatment; photocatalysis; visible light

1. Introduction

Water and soil ecosystems are being degraded because of enormous industrialization and a rise in population. The most significant environmental pollutants are manufactured organic compounds such as pigments, agricultural chemicals, and pharmaceutical products [1,2].

These hazardous pollutants must be thoroughly cleaned before they are released into the ecosystem. Various treatment processes, such as membrane filtration, chemical oxidation, coagulation, adsorption, flocculation, ozonation, and so on, have been employed to eliminate pollutants in the past [3,4]. However, most traditional processes are not environmentally friendly and have drawbacks such as fancy cost, low efficiency, harmful waste concentration, and others [5]. To date, the most exciting treatment technology for removing hazardous dyes and other organic contaminants found in industrial effluent is the Advanced Oxidation Process (AOP). Among the several AOPs, photocatalytic degradation was identified as a promising and cost-effective treatment strategy for reducing environmental issues [6,7]. High oxidizing species, especially $^{\cdot}OH$ and $O_2^{\cdot-}$ Radicals were generated in situ in AOPs. The pollutant molecules are subsequently decomposed into smaller, less toxic compounds via these radicals [8].

Selecting suitable support is a critical step in improving photocatalytic performance. For instance, SBA-15, a silica mesoporous molecular sieve, captured much interest because of its well-

 doi:10.20944/preprints202404.0330.v1

ordered two-dimensional hexagonal structure, significant surface area (600-1100 m^2/g), excellent adsorption capacity, high thermal stability, and, most notably, electron delocalization capacity provided by its framework, which allows it to be picked out rather than any other is chosen over to any other silicate substrate [9–14].

The dye-sensitization operation is applied to extend the active spectrum range of photocatalysts. Transition metal-based dyes are the most suitable compounds for achieving excellent electron transfer to semiconductors. Nevertheless, they are costly and not environmentally friendly, so organic pigments can be used in sensitizing [15–18].

In this trial, SBA-15 does not incorporate a semiconductor; hence, the SBA-15 is sensitized by methylene blue. Methylene blue molecules absorb the light, and the electron in the LUMO reacts with dissolved oxygen to produce radicals necessary to degrade the pollutants in water. This creates a simple, easy-to-manipulate, and cheapest photocatalyst that can degrade the pollutants in water.

2. Experimental

2.1. Preparation and Characterization of the Catalysts

According to Toufaily et al. [19], pure silica SBA-15 was synthesized by a sol–gel method by using Pluronic 123 triblock-copolymer. 4 g of Pluronic 123 was added to 30 mL of H_2O, 120 g of HCl 2M and 10.2 ml of tetraethoxysilane (TEOS) at 40 ^{0}C. The solution was stirred for 45 min, and the resulting gel was aged at 40 ^{0}C for 24 h and finally heated at 100 ^{0}C for 24 h. The solid product was recovered by filtration and then calcinated at 500 ^{0}C for 24h to remove the P123 template.

100mg of SBA-15 was added to the solution of methylene blue at 20ppm and stirred for 24h to achieve total adsorption of methylene blue into SBA-15. After that, the solution was filtered, and SBA-15 was washed with distilled water and dried at 60 ^{0}C. The catalyst obtained was named SBA-15-MB.

2.2. Photocatalytic Experiments

Photocatalytic degradation experiments were carried out in a beaker with a volume of 250 mL, in which a 25 W warm white LED lamp with a wavelength between 400 and 800nm was used as the light source. Methyl orange, tetracycline, and malachite green were selected as the model's pollutants concerning cationic, anionic dyes, and pharmaceuticals. The residual concentration of contaminants was determined using a UV-visible spectrophotometer.

The adsorption experiment of 20 ppm MB by 500 ppm of SBA-15 revealed an adsorption percentage of 95 % after 60 minutes, which indicates full adsorption of methylene solution in the sensitization process of SBA-15.

The leaching of MB from SBA-15 during the photocatalytic experiment was determined by measuring the absorbance of MB in each sample using the UV-Vis spectrophotometer. The leaching in all experiments did not exceed 1ppm (5%).

2.3. Characterization Technics

The obtained samples were characterized by different techniques such as X-ray powder diffraction (XRD), Scanning electron microscope (SEM), Fourier transform infrared (FTIR), and Brunauer–Emmett–Teller (BET). The surface parameters of SBA-15 and SBA-15-MB, such as surface area and pore size, were determined using a micromeritics instrument (Gemini VII). The phase composition and crystal structure were analyzed by X-ray diffraction (XRD) using a Bruker D8 advance diffractometer (Cu source, 40 mA, and λ=1.5418) at a scan rate of 4º/min over a 2θ range of 0-60º. The chemical functional group at the surface of SBA-15 and SBA-15-MB was determined using Fourier transform infrared spectrometry (FT-IR). FT-IR spectra were collected using a Shimadzu instrument with a resolution of 4 cm^{-1}, employing the KBr technique and scanning the spectrum in the 4000-500 cm-1 range. We utilized a scanning electron microscope (SEM) equipped with an energy-dispersive X-ray (EDX) detector to evaluate morphology and structural characteristics. Specifically, the SEM analysis was conducted employing a MIRA3 TESCAN microscope.

 doi:10.20944/preprints202404.0330.v1

3. Results and Discussion

3.1. Characterization of Catalyst

3.1.1. XRD

Figure 1 shows the small-angle XRD patterns of SBA-15 and SBA-15-MB, the scan range of 2 theta degrees of 0.5° to 10°. The typical XRD pattern for SBA-15 and SBA-15-MB exhibits three characteristic peaks relative to the (100), (110), and (200) planes at 2θ of 0.96°, 1.45°, and 1.7°. These peaks characterize the two-dimensional hexagonal structure of SBA-15, which matches SBA-15 synthesized using TEOS as the silica source. The adsorption of methylene blue in the SBA-15 does not affect the crystallinity of SBA-15.

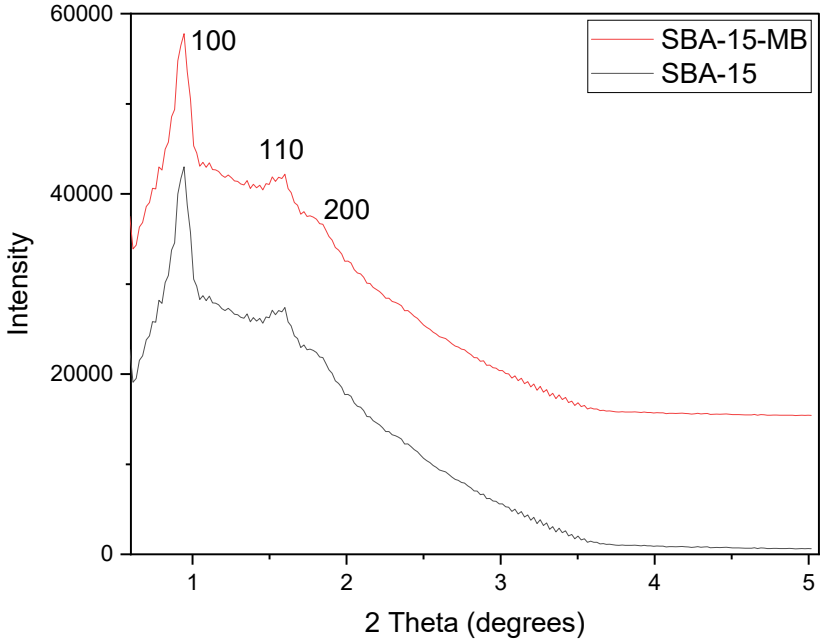

Figure 1. XRD patterns of SBA-15 and SBA-15-MB.

3.1.2. SEM and EDX

Scanning electron microscopy (SEM) equipped with EDX measured the particle morphology and elementary composition. SEM images of the SBA-15 and SBA-15-MB samples are compared in Figure 2. The two images show a spherical morphology of SBA-15. The EDX result shows the presence of carbon in the sample SBA-15-MB, which corresponds to the carbon in the methylene blue molecule and indicates the successful adsorption of methylene blue in the SBA-15.

 doi:10.20944/preprints202404.0330.v1

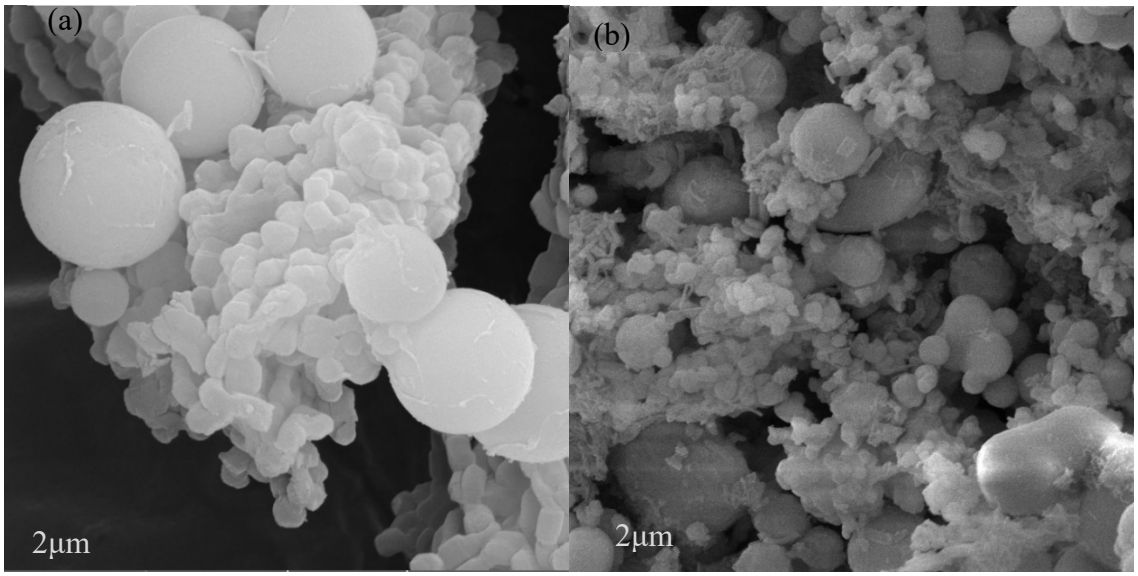

(c)

Elements	% Weight
C	2.46
O	48.56
Si	48.99
Total	100

(d)

Elements	% Weight
C	43.14
O	39.71
Si	17.15
Total	100

Figure 2. SEM image of (a) SBA-15 and (b) SBA-15-MB and EDX for (c) SBA-15 and (d) for SBA-15-MB.

3.1.3. FTIR

The FTIR spectrum of SBA-15 and SBA-15-MB is shown in Figure 3. The peak between 1085 cm^{-1}, characteristic of Si-O-Si bands, indicates the establishment of a condensed silica network, and bands at 803 cm-1 and 456 cm-1 are due to Si-O stretching and bending vibration, respectively. The O-H stretching vibration mode contributed to the large peak at 3400 cm^{-1} [20,21].

The SBA-15-MB composite material still has the prominent characteristic peaks of SBA-15. The characteristic peaks of methylene blue appear in the wavenumber 675-900 cm^{-1} is assigned to the out-of-plane C-H bending vibration of on the benzene ring [22], 1,382 cm^{-1} is given to the symmetric deformation vibration of methyl group, 1,557 cm^{-1} is attributed to the vibration peak of the benzene ring in methylene blue [23], The peak at 1480 cm^{-1} is attributed to $C = C$ stretching vibration. Finally, the peak at 2400 is due to adsorbed MB in SBA-15 [24].

 doi:10.20944/preprints202404.0330.v1

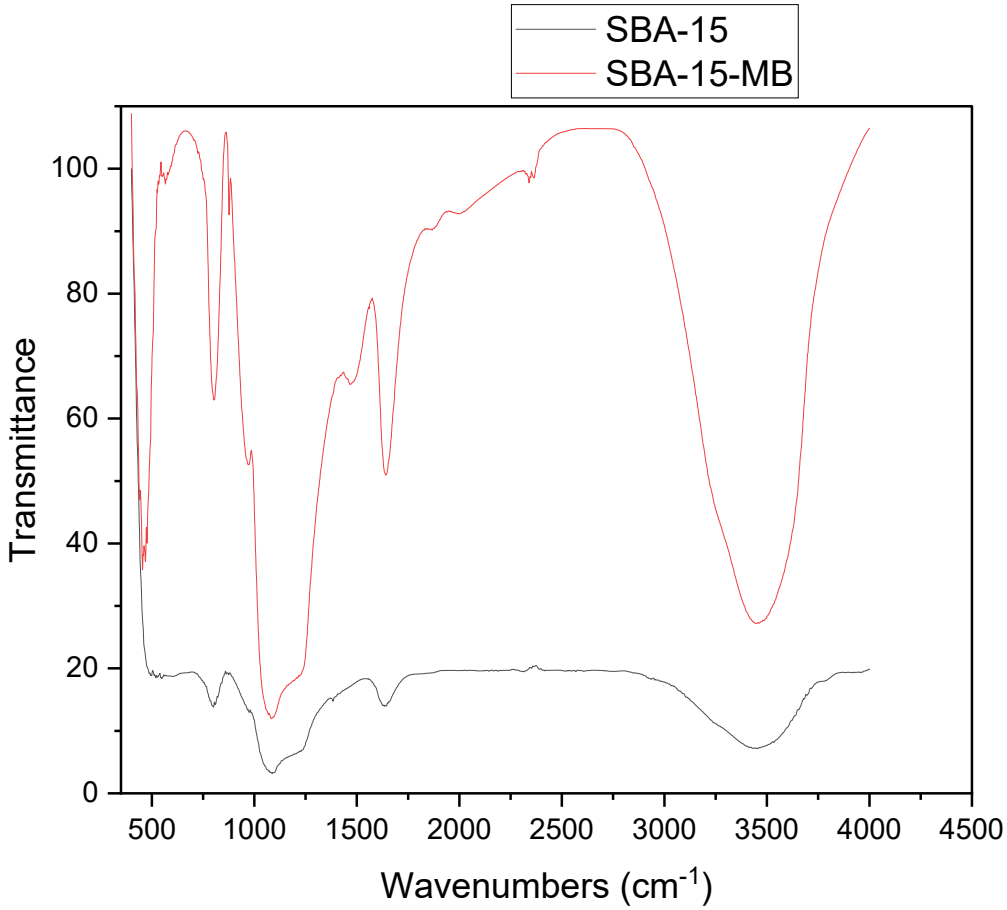

Figure 3. FTIR spectrum of the SBA-15 and SBA-15-MB.

3.1.4. BET

The nitrogen sorption isotherms of both SBA-15 and SBA-16 showed a reduction in the total volume of adsorbed nitrogen after ABZ loading; indicating a significant pore filling of the mesoporous carriers (Figure 4). In addition, SBA-15/ABZ showed a more significant reduction in the pore size than SBA-16/ABZ. Even though the surface area changed, the shape of the isotherms remained the same after drug loading, indicating that the mesoporous texture of carriers was preserved.

Table 1 presents the following textural properties of SBA-15 and SBA-16 before and after drug loading: BET surface area, total pore volume, microporous surface area and micropore volume calculated using the t-plot method and the pore size using the BJH method. BET surface area of SBA-15 and SBA-16 presented similar values. However, the total pore volume of SBA-16 is significantly lower than the total pore volume of SBA-15. After drug loading, decreases in BET surface area, total pore volume, micropore surface area and micropore volume were observed.

Table 1. Values of BET surface area, total pore volume, microporous surface area and micropore volume of SBA-15 and SBA-16.

Sample	S_{BET} (m^2/g)	V_t (cm^3/g)	S_μ[a]	V_μ[b]
SBA-15	692	1	91	0.04
SBA-15-MB	255	0.6	31	0.013

These changes can be explained by the loading of ABZ into pores of mesoporous silica. These results are in good agreement with FT-IR and N2 sorption data indicating that the drug was loaded in the materials. Consequently, in order to quantify the amount of loaded drug in the mesoporous

 doi:10.20944/preprints202404.0330.v1

carriers, elemental analysis was done showing a drug loading of 30.3 wt% and 12.8 wt% for SBA-15 and SBA-16 samples, respectively.

3.2. Photocatalytic Activities of the Photocatalysts SBA-15-MB

To evaluate the photocatalytic activities of the SBA-15-MB photocatalysts, the degradation of methyl orange in water under warm white LED light was investigated. Figure 4 shows the percentage of degradation of methyl orange under 25W warm white LED light. The degradation efficiency of methyl orange reached approximately 80% after 180 minutes. The synthesized SBA-15 shows no adsorption capacity for the MO, which may be because of the negative charge of SBA-15 (pH of zero charge 5 [25]) at pH of methyl orange solution 5.5.

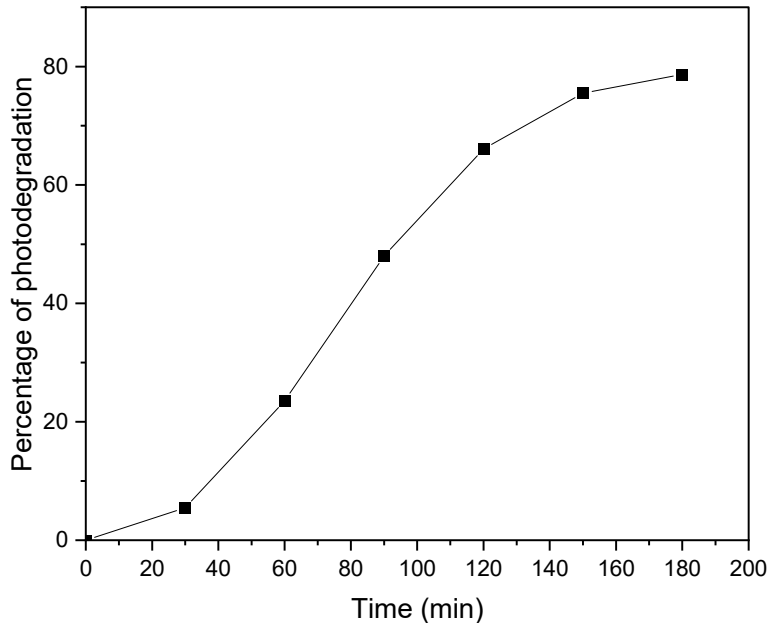

Figure 4. Degradation of methyl orange by SBA-15-MB ([MO]=50ppm, [SBA-15-MB]=300ppm, pH=5.5, 25W LED warm white).

The lamp power's impact on MO degradation (Methylene Blue) is depicted in Figure 5. Notably, while the photodegradation efficiencies at 25 and 50 watts appear similar, the degradation rate at 50 watts surpasses 25 watts. This phenomenon can be attributed to the heightened penetration of photons into the solution at the higher wattage, stimulating a greater number of catalyst particles and subsequently generating more radicals within a given timeframe. Consequently, as the entirety of methylene blue molecules becomes excited, the generation of radicals reaches a saturation point, resulting in comparable degradation efficiencies for 25 and 50 watts after a certain duration.

The study of the efficiency of the SBA-15-MB for the degradation of mix pollutants (MO, MG, TC) with an amount of catalyst 300ppm under 25W warm white LED lamp was mentioned in Table 2.

Preprints.org (www.preprints.org) | NOT PEER-REVIEWED | Posted: 4 April 2024 doi:10.20944/preprints202404.0330.v1

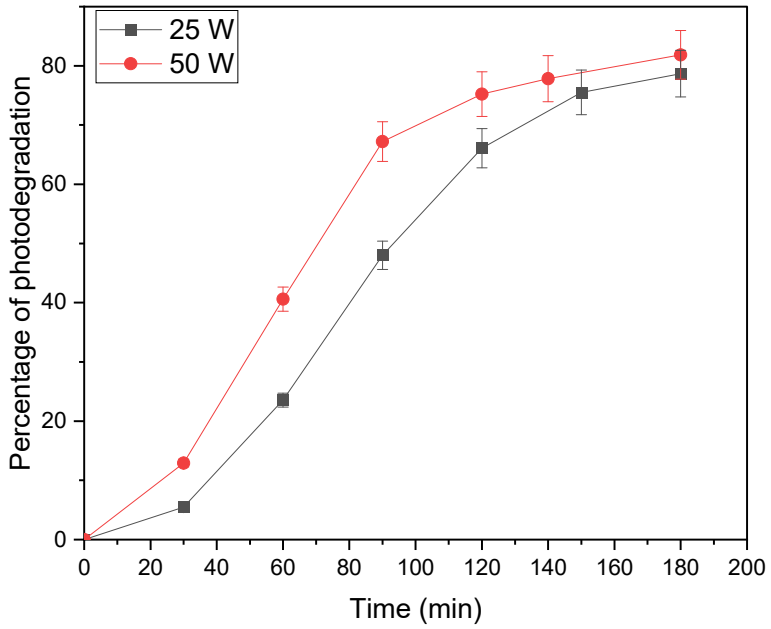

Figure 5. Effect of light power in the degradation of methyl orange by SBA-15-MB ([MO] =50ppm, [SBA-15-MB] =300ppm, pH=5.5).

Table 2. Results of the photodegradation for a mix of pollutants.

Pollutants	MG	MO	TC
Initial concentration in ppm	20	50	20
Percentage of Degradation after 180 min	69	63	38

3.3. Proposed Mechanism of Degradation

When SBA-15-MB is irradiated by visible LED light, the methylene blue is excited, and the electrons are excited from the HOMO levels of the dyes CB to the LUMO levels. Then, the electrons from the LUMO levels can reduce the oxygen to superoxide radicals (see Figure 6. The steps in degrading the dye were proposed using the following equations: [26,27].

$$MB + h\nu \rightarrow MB^{*} \quad (1)$$

$$MB^{*}(e^{-}) + O_2 \rightarrow O_2^{\circ -} \quad (2)$$

$$O_2^{\circ -} + pollutants \rightarrow CO_2 + H_2O \quad (3)$$

$$MB^{+} + O_2^{\circ -} \rightarrow CO_2 + H_2O \quad (4)$$

 doi:10.20944/preprints202404.0330.v1

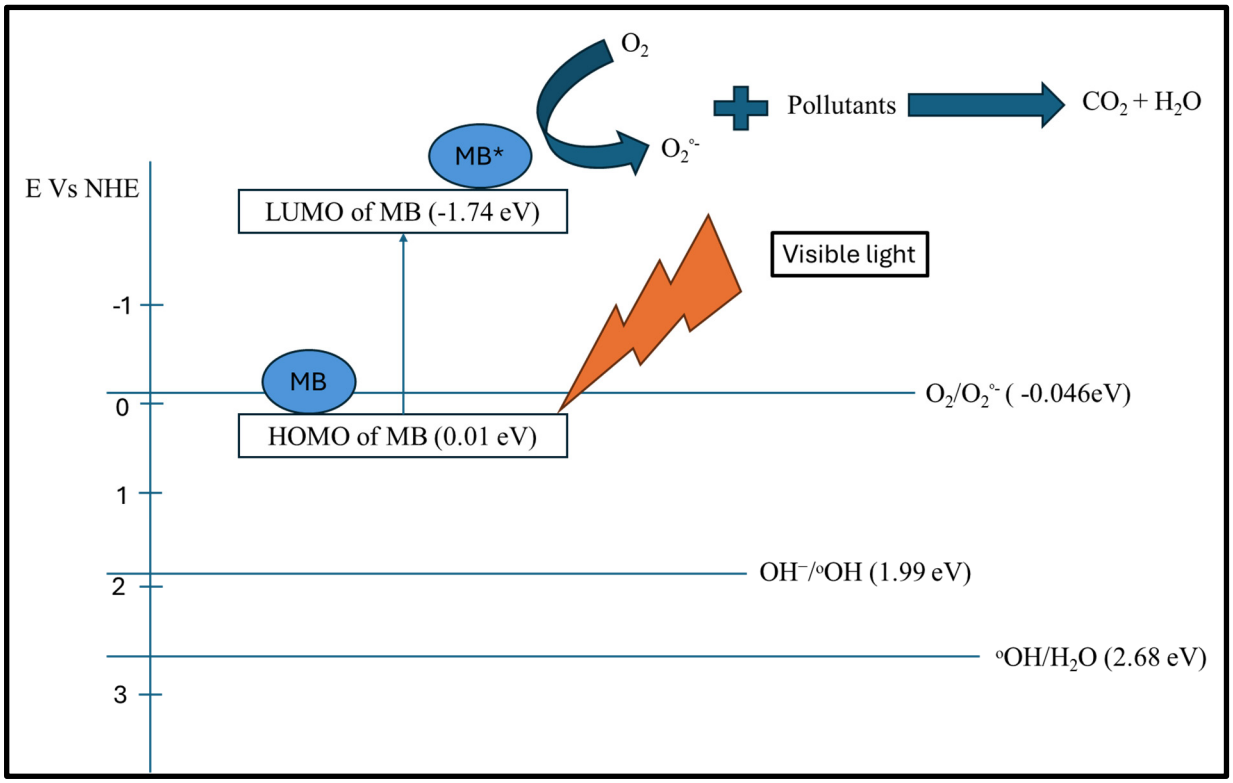

Figure 6. Possible photocatalytic mechanism of SBA-15-MB in the degradation of pollutants.

4. Conclusions

SBA-15 has many advantages for water treatment, such as high surface area, low cost of production, and thermal and chemical stability. The SBA-15 loaded with methylene blue has a low cost, is easy to produce, and has a high photodegradation efficiency against different pollutants, which is a strong possibility for use at an industrial scale to treat effluents. The SBA-15-MB can be prepared by adsorption of MB from effluent, and after that, it can be irradiated to degrade all the pollutants in effluents, including the MB. When the MB adsorbed into SBA was degraded, the SBA-15-MB could be easily regenerated by treatment of effluent containing MB or by adding the SBA-15 to the fresh solution of MB. This catalyst can be examined for other pollutants present in water and other applications such as photodynamic therapy and hydrogen production.

Funding: This research did not receive any specific grant.

Data Availability Statement: There is no additional data.

Conflicts of Interest: The author declares no conflict of interest.

References

1. Qu, X.; Alvarez, P. J. J.; Li, Q. Applications of Nanotechnology in Water and Wastewater Treatment. *Water Res.* **2013**, *47* (12), 3931–3946. https://doi.org/10.1016/j.watres.2012.09.058.
2. Appavu, B.; Thiripuranthagan, S.; Ranganathan, S.; Erusappan, E.; Kannan, K. BiVO4/N-RGO Nano Composites as Highly Efficient Visible Active Photocatalyst for the Degradation of Dyes and Antibiotics in Eco System. *Ecotoxicol. Environ. Saf.* **2018**, *151*, 118–126.
3. Khan, W. Z.; Najeeb, I.; Ishtiaque, S. Photocatalytic Degradation of a Real Textile Wastewater Using Titanium Dioxide, Zinc Oxide and Hydrogen Peroxide. *Int J Eng Sci* **2016**, *5* (7), 61–70.
4. Seow, T. W.; Lim, C. K. Removal of Dye by Adsorption : A Review; 2016.
5. Kanagaraj, T.; Thiripuranthagan, S.; Paskalis, S. M. K.; Abe, H. Visible Light Photocatalytic Activities of Template Free Porous Graphitic Carbon Nitride—BiOBr Composite Catalysts towards the Mineralization of Reactive Dyes. *Appl. Surf. Sci.* **2017**, *426*, 1030–1045.

6. Al-Hetlani, E.; Amin, M. O.; Madkour, M. Detachable Photocatalysts of Anatase TiO2 Nanoparticles: Annulling Surface Charge for Immediate Photocatalyst Separation. *Appl. Surf. Sci.* **2017**, *411*, 355–362. https://doi.org/10.1016/j.apsusc.2017.03.151.
7. Fan, H.-Y.; Shi, C.; Li, X.-S.; Zhang, S.; Liu, J.-L.; Zhu, A.-M. In-Situ Plasma Regeneration of Deactivated Au/TiO2 Nanocatalysts during CO Oxidation and Effect of N2 Content. *Appl. Catal. B Environ.* **2012**, *119–120*, 49–55. https://doi.org/10.1016/j.apcatb.2012.02.016.
8. Kansal, S. K.; Lamba, R.; Mehta, S. K.; Umar, A. Photocatalytic Degradation of Alizarin Red S Using Simply Synthesized ZnO Nanoparticles. *Mater. Lett.* **2013**, *106*, 385–389.
9. Kumaravel, S.; Thiripuranthagan, S.; Radhakrishnan, R.; Erusappan, E.; Durai, M.; Devarajan, A.; Mukannan, A. Liquid Phase Esterification of Levulinic Acid into Ethyl Levulinate over Sulphobenzylated Nanoporous Al-SBA-15 Catalyst. *J. Nanosci. Nanotechnol.* **2019**, *19* (11), 6965–6977.
10. *Synthesis of palladated magnetic nanoparticle (Pd@Fe3O4/AMOCAA) as an efficient and heterogeneous catalyst for promoting Suzuki and Sonogashira cross-coupling reactions - Tamoradi - 2020 - Applied Organometallic Chemistry - Wiley Online Library*. https://onlinelibrary.wiley.com/doi/abs/10.1002/aoc.5538 (accessed 2023-04-23).
11. Veisi, H.; Ozturk, T.; Karmakar, B.; Tamoradi, T.; Hemmati, S. In Situ Decorated Pd NPs on Chitosan-Encapsulated Fe3O4/SiO2-NH2 as Magnetic Catalyst in Suzuki-Miyaura Coupling and 4-Nitrophenol Reduction. *Carbohydr. Polym.* **2020**, *235*, 115966. https://doi.org/10.1016/j.carbpol.2020.115966.
12. Veisi, H.; Tamoradi, T.; Karmakar, B.; Hemmati, S. Green Tea Extract–Modified Silica Gel Decorated with Palladium Nanoparticles as a Heterogeneous and Recyclable Nanocatalyst for Buchwald-Hartwig C–N Cross-Coupling Reactions. *J. Phys. Chem. Solids* **2020**, *138*, 109256. https://doi.org/10.1016/j.jpcs.2019.109256.
13. López-Muñoz, M.-J.; van Grieken, R.; Aguado, J.; Marugán, J. Role of the Support on the Activity of Silica-Supported TiO2 Photocatalysts: Structure of the TiO2/SBA-15 Photocatalysts. *Catal. Today* **2005**, *101* (3–4), 307–314.
14. Ali, A.; Shoeb, M.; Li, Y.; Li, B.; Khan, M. A. Enhanced Photocatalytic Degradation of Antibiotic Drug and Dye Pollutants by Graphene-Ordered Mesoporous Silica (SBA 15)/TiO2 Nanocomposite under Visible-Light Irradiation. *J. Mol. Liq.* **2021**, *324*, 114696.
15. Yun, E.-T.; Yoo, H.-Y.; Kim, W.; Kim, H.-E.; Kang, G.; Lee, H.; Lee, S.; Park, T.; Lee, C.; Kim, J.-H.; Lee, J. Visible-Light-Induced Activation of Periodate That Mimics Dye-Sensitization of TiO2: Simultaneous Decolorization of Dyes and Production of Oxidizing Radicals. *Appl. Catal. B Environ.* **2017**, *203*, 475–484. https://doi.org/10.1016/j.apcatb.2016.10.029.
16. Chowdhury, P.; Athapaththu, S.; Elkamel, A.; Ray, A. K. Visible-Solar-Light-Driven Photo-Reduction and Removal of Cadmium Ion with Eosin Y-Sensitized TiO2 in Aqueous Solution of Triethanolamine. *Sep. Purif. Technol.* **2017**, *174*, 109–115. https://doi.org/10.1016/j.seppur.2016.10.011.
17. (17) Safaralizadeh, E.; Darzi, S. J.; Mahjoub, A. R.; Abazari, R. Visible Light-Induced Degradation of Phenolic Compounds by Sudan Black Dye Sensitized TiO2 Nanoparticles as an Advanced Photocatalytic Material. *Res. Chem. Intermed.* **2017**, *43* (2), 1197–1209. https://doi.org/10.1007/s11164-016-2692-7.
18. Rani, M.; Tripathi, S. K. Electron Transfer Properties of Organic Dye Sensitized ZnO and ZnO/TiO2 Photoanode for Dye Sensitized Solar Cells. *Renew. Sustain. Energy Rev.* **2016**, *61*, 97–107. https://doi.org/10.1016/j.rser.2016.03.012.
19. Toufaily, J.; Koubaissy, B.; Kafrouny, L.; Hamad, H.; Magnoux, P.; Ghannam, L.; Karout, A.; Hazimeh, H.; Nemra, G.; Hamieh, M. Functionalization of SBA-15 Materials for the Adsorption of Phenols from Aqueous Solution. *Cent. Eur. J. Eng.* **2013**, *3*, 126–134.
20. Ahmadi, E.; Dehghannejad, N.; Hashemikia, S.; Ghasemnejad, M.; Tabebordbar, H. Synthesis and Surface Modification of Mesoporous Silica Nanoparticles and Its Application as Carriers for Sustained Drug Delivery. *Drug Deliv.* **2014**, *21* (3), 164–172.
21. Widjonarko, D. M.; Jumina, J.; Kartini, I.; Nuryono, N. Phosphonate Modified Silica for Adsorption of Co (II), Ni (II), Cu (II), and Zn (II). *Indones. J. Chem.* **2014**, *14* (2), 143–151.
22. Belaidi, O.; Bouchaour, T.; Maschke, U. Structural Preferences and Vibrational Analysis of 2-Hydroxy-2-Methyl-1-Phenylpropan-1-One: A Computational and Infrared Spectroscopic Research. *J. Struct.* **2013**, *2013*, e942302. https://doi.org/10.1155/2013/942302.
23. Zhai, Q.-Z.; Dong, Y.; Liu, H.; Wang, Q.-S. Adsorption of Methylene Blue onto Nano SBA-15 Mesoporous Material from Aqueous Media: Kinetics, Isotherms and Thermodynamic Studies. *DESALINATION WATER Treat.* **2019**, *158*, 330–342. https://doi.org/10.5004/dwt.2019.24229.
24. Sabri, A. A.; Albayati, T. M.; Alazawi, R. A. Synthesis of Ordered Mesoporous SBA-15 and Its Adsorption of Methylene Blue. *Korean J. Chem. Eng.* **2015**, *32* (9), 1835–1841. https://doi.org/10.1007/s11814-014-0390-y.
25. Rodríguez-Estupiñán, P.; Legnoverde, M. S.; Simonetti, S.; Díaz Compañy, A.; Juan, A.; Giraldo, L.; Moreno-Piraján, J. C.; Basaldella, E. I. Influence of Functionalization, Surface Area and Charge Distribution of SBA15-Based Adsorbents on CO (II) and NI (II) Removal from Aqueous Solutions. *J. Environ. Chem. Eng.* **2020**, *8* (2), 103671. https://doi.org/10.1016/j.jece.2020.103671.

 doi:10.20944/preprints202404.0330.v1

26. Rtimi, S.; Pulgarin, C.; Sanjines, R.; Kiwi, J. Kinetics and Mechanism for Transparent Polyethylene-TiO2 Films Mediated Self-Cleaning Leading to MB Dye Discoloration under Sunlight Irradiation. *Appl. Catal. B Environ.* **2015**, *162*, 236–244.
27. Li, J.; Zhou, Q.; Yang, F.; Wu, L.; Li, W.; Ren, R.; Lv, Y. Uniform Flower-like BiOBr/BiOI Prepared by a New Method: Visible-Light Photocatalytic Degradation, Influencing Factors and Degradation Mechanism. *New J. Chem.* **2019**, *43* (37), 14829–14840.